Machine Learning-Based in-Band OSNR Estimation From Optical Spectra

Fabiano Locatelli, Konstantinos Christodoulopoulos, Michela Svaluto Moreolo, *Senior Member, IEEE*, Josep M. Fàbrega, *Senior Member, IEEE*, and Salvatore Spadaro, *Senior Member, IEEE*

***Abstract*— Measuring the optical signal to noise ratio (OSNR) at certain network points is essential for failure handling, for single connection but also global network optimization. Estimating OSNR is inherently difficult in dense wavelength routed networks, where connections accumulate noise over different paths and tight filters do not allow the observation of the noise level at signal sides. We propose an in-band OSNR estimation process, which relies on a machine learning (ML) method, in particular on Gaussian process (GP) or support vector machine (SVM) regression. We acquired high-resolution optical spectra, through an experimental setup, using a Brillouin optical spectrum analyzer (BOSA), on which we applied our method and obtained excellent estimation accuracy. We also verified the accuracy of this approach for various resolution scenarios. To further validate it, we generated spectral data for different configurations and resolutions through simulations. This second validation confirmed the estimation quality of the proposed approach.**

***Index Terms*— Machine learning, optical performance monitoring, optical signal to noise ratio, optical spectrum.**

I. Introduction

THE optical signal to noise ratio (OSNR) is considered one of the most important signal quality parameters to measure. It is transparent to the bit rate and modulation format and it can be easily correlated to the bit error rate (BER) [1]. One of the most common method to measure the OSNR employs optical spectrum analyzers (OSAs) [2]. By interpolating the noise level at the sides of the considered channel, the OSA allows the measurement of the amplified spontaneous emission (ASE) noise introduced by the optical amplifiers and other noise-sensed impairments. Such measurements are typically taken *offline* to optimize a newly deployed connections or for troubleshooting failures.

Issues arise in wavelength switched optical networks employing ultra-dense wavelength division multiplexing (ultra-DWDM) or flex-grid filters [3]. In such networks, the channels exhibit different noise levels, according to their routes. Furthermore, a connection along its path crosses certain reconfigurable optical add/drop multiplexers (ROADMs), which employ optical filters. The filters introduce a sharp power drop between the channels, making the measurement of the noise level challenging [4]. Figure 1 shows two acquisition examples of filtered channels where it is apparently difficult to identify the noise level. Another issue is the filter cascade effect (FCE): after several filters the pass-band tightens, distorting the signal and making even harder the identification of the noise level [5]. Thus, measuring the OSNR has to be done in-band [3]. Since the introduction of coherent receivers polarization multiplexed (PM) channels are mostly used, making polarization nulling techniques for measuring OSNR unsuitable. A method is to establish the connection, measure the signal and turn it off to measure its noise. However, this cannot be done while the network is operating. Failure handling and dynamic network optimization in low margin and/or in disaggregated networks requires to measure the OSNR in-band and non-intrusively, as the network operates [6], [7].

Nowadays, very high-resolution optical spectrometry equipment are available, as for example the Brillouin optical spectrum analyzer (BOSA) [8]. This device exploits the stimulated Brillouin scattering (SBS), a non-linear optical effect that causes a very narrow filtering [9], which allows the BOSA to achieve spectral resolutions up to 0.1 pm (12.5 MHz). On the other hand, the classic OSAs range in the order of 0.01 nm (1.25 GHz) [10]. Authors in [11] proposed to use a high-resolution spectrum analyzer for in-band OSNR monitoring. However, such equipment is bulky and expensive, thus hard to be used in deployed networks, in the wild. Much cheaper and less accurate solutions, referred to as channel monitors [12], have also recently become available, and could potentially be used for in-band OSNR monitoring at ROADM nodes. However, it is unclear which spectral resolution and what processing method must be used to achieve good accuracy.

Machine learning (ML) has recently been adopted in several scientific fields and is also becoming attractive in optical communications. In [13], the authors considered four common ML models, and in particular, support vector machine (SVM), artificial neural network (ANN), k-nearest neighbors (KNN)

Manuscript received August 4, 2019; revised September 27, 2019; accepted October 21, 2019. Date of publication October 29, 2019; date of current version December 19, 2019. This work was partially funded by the ONFIRE (Future Optical Networks for Innovation, Research and Experimentation) project supported by EU Horizon 2020 Research and Innovation Programme under the Marie Skłodowska-Curie grant agreement No. 765275. *(Corresponding author: Fabiano Locatelli.)*

F. Locatelli is with the Nokia Bell Labs, 70435 Stuttgart, Germany, and also with the Centre Tecnològic de Telecomunicacions de Catalunya, Optical Networks and Systems Department, 08860 Castelldefels, Spain (e-mail: fabiano.locatelli@cttc.es).

K. Christodoulopoulos is with the Nokia Bell Labs, 70435 Stuttgart, Germany (e-mail: konstantinos.1.christodoulopoulos@nokia-bell-labs.com).

M. S. Moreolo and J. M. Fàbrega are with the Centre Tecnològic de Telecomunicacions de Catalunya, Optical Networks and Systems Department, 08860 Castelldefels, Spain (email: michela.svaluto@cttc.es; josep.maria.fabrega@cttc.es).

S. Spadaro is with the Department of Signal Theory and Communications, Universitat Politecnica de Catalunya (UPC), 08034 Barcelona, Spain (e-mail: spadaro@tsc.upc.edu).

Color versions of one or more of the figures in this letter are available online at http://ieeexplore.ieee.org.

Digital Object Identifier 10.1109/LPT.2019.2950058

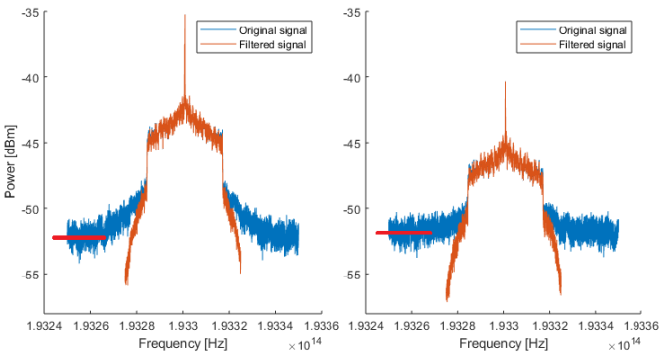

Fig. 1. Optical spectra before (blue) and after (orange) the 50 GHz-bandwidth filter captured at high-resolution (0.1 pm) in the experimental setup. The red lines indicate the noise level floor.

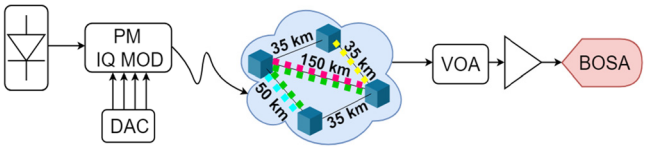

Fig. 2. Schematic diagram of the experimental setup for the high-resolution optical spectra acquisition. PM-IQ-MOD: polarization multiplexed-IQ-modulator, DAC: digital-to-analog converter, VOA: variable optical attenuator, BOSA: Brillouin optical spectrum analyzer.

and decision tree, and identified SVM as the most promising approach for OSNR estimation. However in [13], most of the spectral data were generated with a simulation tool and only few with experiments. Moreover, they considered classification with 1 dB accuracy, which is rather coarse, depending on the use case at hand. Finally, they processed wide and not in-band spectrum, which is not available in deployed filtered networks.

In this letter, we propose a method that, despite the aforementioned challenges, estimates accurately the OSNR from the in-band optical spectrum in short-distance scenarios. For longer distance applications, the contribution of nonlinearities should be also considered [14]. We used a BOSA to capture high-resolution experimental spectral data, and in turn train two ML regression methods for estimating in-band OSNR: a Gaussian Process (GP) and an SVM model. Relying on high resolution optical spectra theoretically allows the identification of the channel noise level more precisely than a standard OSA [6]. To evaluate the effect of the resolution on the estimation accuracy, we applied the same methods with lower-resolution spectral input. Finally, we carried out a further validation of the proposed ML-based process using simulation-generated optical spectra with different modulation formats and various filter and noise scenarios. The proposed GP ML method achieved a maximum error of 1.1 dB in all the experimental scenarios, where OSNR ranged from 10 to 30 dB, and a maximum error of 0.3 dB in all the simulated scenarios, where OSNR ranged from 22 to 35 dB. Also, we did not observe any deterioration of accuracy for resolutions up to 1.25 GHz.

II. Experimental Setup and Spectral Processing

Figure 2 depicts the experimental setup used to capture several high-resolution optical spectra. We generated a 28 GBd polarization multiplexed-quadrature phase shift keying (PM-QPSK) modulated signal, with a tunable laser working at 1550.918 nm. No pulse shaping was used. We obtained back to back (B2B) measurements and transmitted the signal over 4 different distance paths: 35 km, 50 km, 150 km and 200 km, using the ADRENALINE testbed. At the output of the testbed, we placed a variable optical attenuator (VOA) and then an erbium-doped fiber amplifier (EDFA) operating at constant power to emulate more spans and obtained 16 different OSNR levels. Finally, we acquired the spectra using the BOSA. For each scenario, we collected a total of 160 optical spectra, specifically 10 for each VOA level (5 for each polarization state). The optical signal passes through an optical filter when entering and through another when exiting the ADRENALINE testbed: the 35 km and 50 km scenarios had entry/exit optical filters with 100 GHz-bandwidth, while the 150 km and 200 km cases, had 100 GHz entry and 50 GHz-bandwidth exit filter.

We then processed the collected spectra. During this phase, we applied a 50 GHz-bandwidth optical filter to the acquired spectra. This was done so as to create a variety of possible realistic network conditions, such as: laser drift and filter tightening, by misaligning the filter with the laser and reducing the size of the filter, respectively. Then after applying the filter, we cut the spectra at the filter edges to replicate a real DWDM spectrum, where each channel is bounded by its adjacent, thus resulting in a narrow area for measuring the OSNR. Figure 1 shows examples of high-resolution filtered optical spectra together with their original pre-filtered versions. As expected, the filter removes information at the sides of the channel, making sometimes infeasible to identify the noise actual level.

We represent the acquired optical spectrum with the vector $\boldsymbol{s}$ of length n. The length n depends on the equipment spectral resolution r (GHz) and on the network allocated bandwidth b (GHz), which corresponds to the configuration of the filters along the path, so that $n = b/r$. When measuring with the BOSA at high-resolution ($r = 12.5$ MHz) and for a filter bandwidth $b = 50$ GHz, the length n was equal to 4000. To examine the accuracy of the proposed OSNR estimation method, described in the next Section, in the case of an OSA or a channel monitor, i.e. with a resolution of $r = 1.25$ GHz, we post-processed the collected high-resolution spectra to create low-resolution versions. To do so, we averaged the spectra in the linear domain, reducing their length to $n = 40$. Theoretically, we expect a higher accuracy with higher-resolution. We then associated each spectrum $\mathbf{s}$ to its reference OSNR value y, which was calculated through the integral method on the high-resolution spectra before the filter application. Spectra with OSNR reference values lower than 8 dB were excluded a priori from further processing, since in real systems such low OSNR signals would not be kept in operation.

III. Proposed ML OSNR Estimator

Our goal is to find the mapping f between the connection's spectrum $\boldsymbol{s}$ and its OSNR value y, that is $y = f(\boldsymbol{s})$. We denote with the matrix $\boldsymbol{S_c}$, of dimensions $n \times m$, the set of m collected spectra of signals with the same parameters $c = (r, b, q)$, where r is the spectral resolution, b is the filtered

bandwidth and q is the connection symbol rate. We also denote by vector $\boldsymbol{y_c}$, of length m, their reference OSNR values. To approximate the estimation function f, we implemented a ML model Q_c specific for channels with parameters c. Thus, we trained Q_c with the sets $(\boldsymbol{S_c}, \boldsymbol{y_c})$ as input. Let $\hat{\boldsymbol{y}}_{\boldsymbol{c}} = Q_c(\boldsymbol{S_c})$ be the estimated OSNR values and $\boldsymbol{\varepsilon_c} = \hat{\boldsymbol{y}}_{\boldsymbol{c}} - \boldsymbol{y_c}$ the estimation error. The goal of training is to identify Q_c so as to minimize some function of the estimation error $\boldsymbol{\varepsilon_c}$, for example the mean squared error (MSE).

SVM and GP are two nonparametric ML techniques for classification and regression, which rely on kernel functions. We formulated the estimation as a regression problem and we trained the SVM and GP models using the linear and the squared exponential kernel functions, respectively.

As mentioned, for each path and VOA configuration in the testbed, we collected a total of 10 spectra, 5 for each polarization state. To improve the quality of the considered spectral data, we first time-averaged the 5 spectra of each polarization state, and added up the 2 resulting spectra. Indeed, time averaging is a typical process to reduce the monitoring errors and the randomness of Gaussian effects. Furthermore, to reduce the effect of a laser drift, we identified the channel central frequency of each spectrum (detecting the peak relative to the carrier) and re-aligned it based on that.

The proposed ML-based estimation method requires for training the reference OSNR values. We described above how we obtained the reference OSNR values in the testbed. In operating networks, assuming deployed channel monitors at the nodes, we could measure the in-band OSNR of PM signals with the On/Off method [3] during their provisioning, before the channel operates. We can make use of the SNR monitored at the DSP of the coherent receiver after making certain assumptions and converting it to OSNR. We can also perform experiments in the lab to complement the above. Once the ML algorithm is trained with the spectra $\boldsymbol{S}_c$ and their reference OSNR values $\boldsymbol{y}_c$, it estimates the OSNR $\hat{y}$ of an operating channel with the same parameters c, assumed to be known by the control plane, from its spectrum $\boldsymbol{s}$.

IV. Results and Discussion

We evaluated the estimation performance of the proposed ML method (Section III) using the high resolution spectra acquired in the experimental setup (Section II). To be more specific, all acquired spectra comprised the set $\boldsymbol{S_c}$ with parameters $c = (r = 12.5$ MHz, $b = 50$ GHz, $q = 28$ GBd). The total number of spectra m was 198, and we used the ∼85% (169) of these to train the algorithm, whereas the remaining ∼15% (29) for testing it. To evaluate the estimation accuracy, we randomly shuffled the training and testing sets 200 times, trained a different ML model each time and tested it with the corresponding sets. In the first part of this section we report the results of the best performing ML model, which was GP.

Figure 3 shows the reference and the estimated OSNR values for the 50 km path distance scenario as a function of the different VOA levels. We trained the GP ML model with the high resolution spectra training set with all the path distances (and B2B) and plot the spectra of the 50 km signals from the testing set. Figure 4 shows the probability

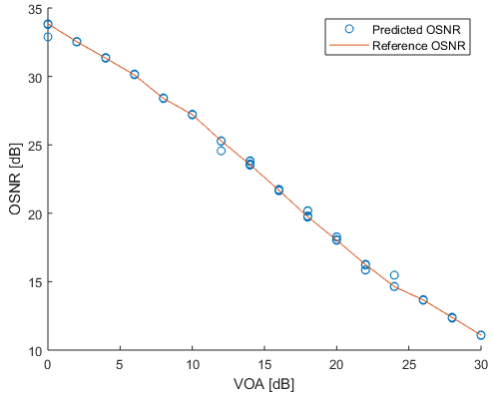

Fig. 3. Reference and predicted OSNR values as function of the VOA levels for the 50 km distance scenario.

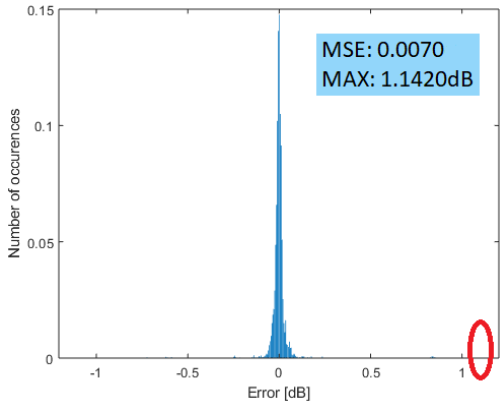

Fig. 4. Probability density function of the OSNR estimation error of the GP model and high-resolution spectra. The maximum error is highlighted in the red circle.

density function (PDF) of the error made by the GP with respect to the reference for the high-resolution optical spectra. As highlighted in the figure inset, the mean squared error (MSE) was 0.0070 dB and the maximum error (MAX) was 1.1420 dB. The accuracy achieved with the low-resolution spectra (which correspond to different parameters c and a different trained model Q_c), were identical to those of the high-resolution case. Therefore, concerning the experimental acquired optical spectra, no difference arose between the two resolution versions. We did not observe any dependence of the estimation error with respect to the reference OSNR in the range between 10 dB to 30 dB of the experimentally acquired data. It is worth noting that the reference OSNR and the spectra used in the ML method were acquired with a state of the art measuring equipment (BOSA) with a dynamic range of $>$ 80 dB.

For a further validation, we carried out several VPI-based simulations and collected additional sets of optical spectra. Figure 5 shows the VPI simulation setup. We created a 28 GBd PM-QPSK signal with roll-off factor $\alpha = 1$, yielding a 112 Gb/s connection. A second order Gaussian optical filter was used to emulate the effect of passing through a number of ROADMs. We considered 16 VOA levels and a filter with 37.5 GHz bandwidth. In addition, we modified

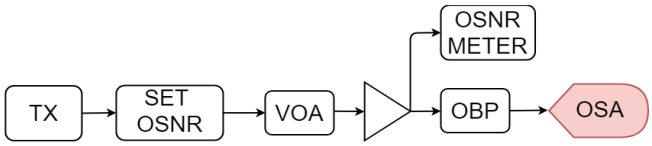

Fig. 5. Schematic diagram of the VPI simulation setup. TX: optical transmitted signal, VOA: variable optical attenuator, EDFA: erbium-doped fiber amplifier, OBP: optical bandpass filter, OSA: optical spectrum analyzer.

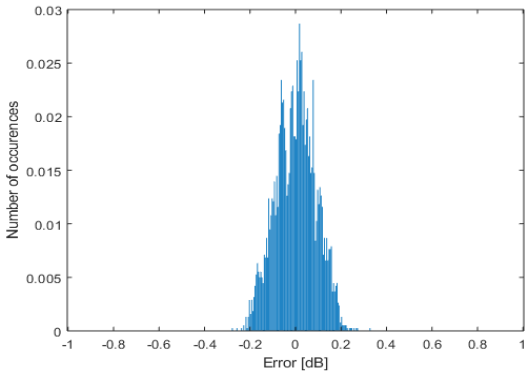

Fig. 6. Probability density function of the error committed by the GP while predicting the OSNR using PM-16QAM as modulation format for the high-resolution VPI simulated spectra.

TABLE I
SUMMARY RESULTS FOR THE SIMULATED OPTICAL SPECTRA

Modulation format	*Optical filter bandwidth [GHz]*	*Optical spectral resolution*	*MSE* ($\times 10^{-3}$)		*MAX [dB]* ($\times 10^{-3}$)	
			GP	*SVM*	*GP*	*SVM*
PM-QPSK	37.5	0.1 pm	8.5	21.6	212	495
		0.01 nm	6	8.7	260	315
PM-16QAM	37.5	0.1 pm	7.7	20.2	327	547
		0.01 nm	3.9	16.3	186	552

the filter central frequency and bandwidth to emulate two realistic scenarios: filters shift/laser drift ($\pm$ 1 GHz), and FCE (reducing the 37.5 GHz filter to 25 GHz). We collected the spectral data by an OSA-VPI module with 0.1 pm and 0.01 nm resolutions, and in total we acquired 96 optical spectra for each resolution. Exploiting the same VPI setup, we also generated a 224 Gb/s PM-16QAM signal with again a 37.5 GHz filter configuration and collected 128 spectra for each resolution scenario. In total we created four sets of spectra according to the related parameters c: high and low-resolution for PM-QPSK and PM-16QAM. As before, for each set we used 85% of the spectra for training and the 15% for testing. We shuffled the spectra of each set 200 times, each time we trained, estimated, and obtained the errors. Figure 6 shows the estimation error PDF with high-resolution spectra and the PM-16QAM channel. We summarize all the results for both the ML models in Table I. We observed a maximum OSNR estimation error lower than 0.4 dB in all the considered scenarios. Again, as in the experimental results, minor deviations were observed when comparing the two resolution versions of the spectra.

Future steps involve the deployment of a new experimental setup that will include optical filters and a coherent OSA (150 MHz resolution) and/or channel monitors to collect the optical spectra. We will verify the performance of our proposed method in such a more realistic setup. We would also examine the generality of the created models and the dependence on specific transmission parameters, e.g. train the ML with spectra of a specific set of parameters (e.g. modualtion format or roll-off factor), and test it with spectra of different parameters.

V. Conclusion

We developed a machine learning-based in-band OSNR estimator, relying on GP or SVM models. We evaluated its estimation accuracy with experimental and simulation generated spectra. The results showed an excellent accuracy of the proposed process, a maximum error of 1.1 dB in experimental and 0.3 dB in simulated scenarios.

Acknowledgment

The authors would like to thank Aragon Photonics Labs for providing the BOSA used for the experiments.

References

[1] C. C. K. Chan, *Optical Performance Monitoring*. Burlington, MA, USA: Elsevier, 2010.
[2] *Optical Signal-to-Noise Ratio Measurement for Dense Wavelength-Division Multiplexed Systems*, Standard IEC 61280-2-9, 2009.
[3] *Fibre Optic Communication System Design Guides—Part 12: In-Band Optical Signal-to-Noise Ratio (OSNR)*, Standard IEC TR 61282-12, 2016.
[4] A. Morea, J. Renaudier, T. Zami, A. Ghazisaeidi, and O. Bertran-Pardo, "Throughput comparison between 50-GHz and 37.5-GHz grid transparent networks [invited]," *J. Opt. Commun. Netw.*, vol. 7, no. 2, pp. A293–A300, Feb. 2015.
[5] J. M. Fàbrega *et al.*, "On the filter narrowing issues in elastic optical networks," *IEEE/OSA J. Opt. Commun. Netw.*, vol. 8, no. 7, pp. A23–A33, Jul. 2016.
[6] Viavi Whitepaper. (2915). *In-Band OSNR Measurements on 40 G Polarization-Multiplexed QPSK Signals Using a Field-Deployable, High-Resolution OSA*. [Online]. Available: https://www.viavisolutions.com/en-us/literature/band-osnr-measurements-40-g-polarization-multiplexed-qpsk-signals-using-field-deploy-white-paper-en.pdf
[7] Z. Huang *et al.*, "A novel in-band OSNR measurement method based on normalized autocorrelation function," *IEEE Photon. J.*, vol. 10, no. 2, Apr. 2018, Art. no. 7903208.
[8] A. Photonics. *BOSA Technology*. Accessed: Jul. 2019. [Online]. Available: https://aragonphotonics.com/bosa/
[9] J. M. S. Domingo, J. Pelayo, F. Villuendas, C. D. Heras, and E. Pellejer, "Very high resolution optical spectrometry by stimulated Brillouin scattering," *IEEE Photon. Technol. Lett.*, vol. 17, no. 4, pp. 855–857, Apr. 2005.
[10] J. M. Fàbrega, M. S. Moreolo, and L. Nadal, "Optical performance monitoring systems in disaggregated optical networks," in *Proc. 20th Int. Conf. Transparent Opt. Netw.*, Jul. 2018, pp. 1–4.
[11] W. Moench and E. Loecklin, "Measurement of optical signal-to-noise-ratio in coherent systems using polarization multiplexed transmission," in *Proc. Opt. Fiber Commun. Conf. Exhib.*, Mar. 2017, pp. 1–3.
[12] (2015). *Flexgrid High Resolution Optical Channel Monitor (OCM)*. Finisar, Sunnyvale, CA, USA. [Online]. Available: https://www.finisar.com/sites/default /files/downloads/flexgrid_high_resolution_ocm_pb_web.pdf
[13] D. Wang *et al.*, "Machine learning-based multifunctional optical spectrum analysis technique," *IEEE Access*, vol. 7, pp. 19726–19737, 2019.
[14] M. Lonardi *et al.*, "Optical nonlinearity monitoring and launched power optimization by artificial neural networks," in *Proc. Eur. Conf. Opt. Commun.*, Sep. 2019, pp. 1–4.